A innovative model for the plume simulation of electric thrusters

IEPC-2017-313
Presented at the 35thInternational Electric Propulsion Conference
Georgia Institute of Technology • Atlanta, Georgia • USA
October 8 – 12, 2017

Yong Cao[1]， Pei Qiu[2] ， Chang Lu[3] and Yuchuan Chu[4]
Harbin Institute of Technology, Shenzhen Graduate School, Guangdong 518055, People's Republic of China

Abstract: CEX ion is the main factor causing the plume pollution. The distribution of CEX ions is determined by the distribution of beam ions and neutral atoms, so the primary problem in the study of plume is how to accurately simulate the distribution of beam ions and neutral atoms. At present, the most common-used model utilized for the plume simulation is the analytical model proposed by Samanta Roy for the plume simulation of NSTART ion thruster. However, this analytical model can only be applied to the ion beams with the small divergence angle. In addition, the analytical model is no longer applicable to the simulation of the plume of a new type of ion thruster appeared recently, which is called the annular ion thruster. Therefore, in this paper, a 3D full particle model is proposed for the plume simulation of ion thrusters consisting of Particle model for the ion beam, DSMC model for the neutral atoms and IFE-PIC-MCC model for CEX ions. Then the plume in the NSTAR ion thruster is simulated by both Roy's model and the3D full particle model. The simulation results of both models are compared to the experimental results. Finally, we simulated the plume of the annular ion thruster using the 3D full particle model. Results indicate that this 3D full particle model is well agreement with the analytical model and experimental data, and it can also be used for other electric thrusters.

I. Introduction

AS the advantages of electric thruster such as small size and large specific impulse, the electric thruster is being widely used in the field of satellite communications and deep space exploration. But in practical application, it is found that electric thruster plume will bring great harm to the spacecraft, and even lead to spacecraft failure. For example, the CEX ion in the plume can bring harmful forces and thermal loads and pollute the electronic components of the aircraft[1-3]. Therefore, how to reduce or circumvent the impact of electric thruster plume on spacecraft is critical to the future application of electric thruster. The research methods of electric thruster plume mainly include experimental and numerical simulation. The experiment is time-consuming and expensive. Conversely, numerical simulation is

[1]Associate Professor, Department of Mechanical Engineering Automation, Shenzhen Graduate School; yongc@hit.edu.cn
[2]Master Candidate, Department of Mechanical Engineering Automation, Shenzhen Graduate School; qiupeihit@outlook.com
[3]Ph.D. Candidate, Department of Mechanical Engineering Automation, Shenzhen Graduate School; luchang@stmail.hitsz.edu.cn
[4]Postdoctoral Fellow, Department of Mechanical Engineering Automation, Shenzhen Graduate School; ychuan.chu@hitsz.edu.cn

economic and well-adapted, and a further comprehensive understanding of the distribution of plumes can be got, which has been widely used.

The composition of the electric thruster plume consists mainly of beam ions, neutral atoms, and CEX ions[4]. The distribution of CEX ion is determined by the distribution of beam ions and neutral atoms. Therefore, how to accurately simulate the distribution of beam ions and neutral atoms is the primary problem of numerical simulation. The mature models simulating the distribution of beam ions and neutral atoms include analytical model and full particle model. The analytical model proposed by R. I. Samanta Roy[5] is one of the current matures simulation models of ion thruster plume. In this model, the beam distribution formula is based on the experimental data. The distribution of neutral atoms is based on the point source model proposed by Bird[6]. And the CEX collision is simulated by Stand MCC. Wang[7] et al. simulated the plume of NSTAR ion thruster based on the combination of analytical model and IEF algorithm, and compared the simulation results with experimental data. The results show that the simulation results of the analytical model are in good agreement with the experimental data. The analytic model has the advantages of fast calculation and good agreement with the experimental results, but for the case where the divergence angle is too large, or for the plume of annular ion thruster[8] and other electric thruster plumes, the analytic model is no longer applicable. With the development of electronic technology, computer performance improves rapidly. So the simulated particles of the full particle model can be up to 10^9, and the calculation accuracy also therefore greatly improves. However, the full particle model is mainly proposed for Hall thrusters[9-11], so there is no systematic comparison validation for the full particle model applicable for plume of ion thruster and its correctness and accuracy.

Therefore, this paper presents a 3D full particle model for plume of ion thruster, including Particle model of beam ions, DSMC model of neutral atoms and IFE-PIC-MCC[12-15] model of CEX ions, and then compares the 3D full particle model with the analytical model and the experimental data to verify its correctness and accuracy. On this basis, this paper simulates the plume of annular ion thruster. In the second chapter, we introduce the beam ion sub-model of the analytical model and the 3D full particle model, and then compare the beam ion simulation results of this two models. In the third chapter, we introduce the CEX ions simulation process of the analytical model and the 3D full particle model, and compare the simulation results of the two models with experimental data of the NSTAR ion thruster plume. In the fourth chapter, we simulate the plume of the annular ion thruster recently emerging. The results show that the simulation results of the 3D full particle model are in good agreement with the simulation results of the analytical model and the experimental data. Moreover, the model is applicable for the simulation of the electric thruster plume of annular ion thruster and Hall thruster. In addition, based on the advantages that the IFE algorithm can quickly deal with complex boundaries in the structured mesh, the model also has the potential to calculate non-axisymmetric plumes and to directly calculate the interaction between plume CEX ions and complex surfaces of spacecraft.

II. Beam ion simulation model

In the Particle model of beam ion, this paper presents the central distribution of the initial position of th e beam ion based on the analytical model. Therefore, this section first reviews the analytical model of beam ion, and then introduces the Particle model in detail, and finally compares the beam ion simulation results of analytical model and Particle model.

(1) Analytical model

As shown in Fig. 1, the beam ion distribution is subject to the point source model. The beam ions are e mitted from the point source of the center of sphere of optics, and the beam current density j_{bi} is subject to the parabola distribution near the axis, and is subject to the exponential distribution in the wing area. The p olar coordinate distribution Equation is shown in Eq. (1)[5]。

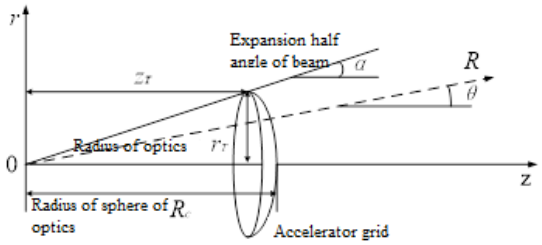

Figure 1. Schematic diagram of beam point source model

$$j_{bi}(R,\theta)=\begin{cases} ev_{bi}n_{bi0}(\frac{R_c}{R})^2(1-\frac{\theta^2}{\alpha^2}), \theta<\gamma\alpha \\ ev_{bi}n_{bi0}\exp(-\frac{R\cdot\sin\theta}{\lambda})(\frac{R_c}{R})^2(1-\frac{\theta^2}{\alpha^2}), \theta\geq\gamma\alpha \end{cases} \quad (1)$$

Where, e is the quantity of electron charge; α is the divergence angle of the beam; θ is the angle between the straight line of the arbitrary point and the center of the sphere and the outlet axis of the thruster, when $\theta<\gamma\alpha$, it is the core area of the beam; when $\theta\geq\gamma\alpha$, it is the wing area, the beam current density decreases by $\exp(-\frac{R\cdot\sin\theta}{\lambda})$, and, typically, γ is valued as 0.95; R is the distance between the arbitrary point and the center of sphere, where R_c is the radius of sphere of optics, $R_c\approx r_T/\alpha cos(\alpha/2)$, and r_T is the radius of optics; n_{bi0} is the density at the central point of outlet of the beam ion; v_{bi} is the beam ion velocity, which is assumed as constant:

$$v_{bi}=\sqrt{\frac{2eU_{acc}}{m_i}} \quad (2)$$

Where, U_{acc} is the accelerating voltage of optics, and m_i is the beam ion mass.

In the analytical model, the initial parameters needed to be determined when solving the beam ion distribution are v_{bi} and n_{bi0}. v_{bi} has been obtained by the Eq. (2), and n_{bi0} can be obtained according to the beam current conservation.

The beam of the any spherical surface outside the outlet of the thruster shall meet:

$$I_b=\int_0^{\alpha} j_{bi}2\pi R^2\sin\theta d\theta \quad (3)$$

Since the wing area is very narrow and the beam current density of the wing area is also very small, this part of area is ignored in Eq. (3). Substitute the part of $\theta<\gamma\alpha$ in Eq. (1) into Eq. (3) and obtain:

$$I_b=2\pi ev_{bi}n_{bi0}R_c^2\cdot(1-\frac{2\cos\alpha}{\alpha^2}-\frac{2\sin\alpha}{\alpha}+\frac{2}{\alpha^2}) \quad (4)$$

Substitute $R_c\approx r_T/\alpha cos(\alpha/2)$ into Eq. (4) and obtain:

$$I_b=\pi ev_{bi}n_{bi0}r_T^2\frac{2(\alpha^2-2\cos\alpha-2\alpha\sin\alpha+2)}{\alpha^4\cos^2(\alpha/2)} \quad (5)$$

Let $\delta(\alpha)=\frac{4(\alpha^2-2\cos\alpha-2\alpha\sin\alpha+2)}{\alpha^4\cos^2(\alpha/2)}$, when $\alpha<<1$, $\delta(\alpha)\approx 1$, and then

$$n_{bi0} = \frac{2I_b}{ev_{bi}\pi r_T^2} \quad (6)$$

2）Particle model

After the beam ion enters the plume field, the impact of the electromagnetic field of the plume on the be am ions is negligible due to its high speed. Thus, the motion of the beam ion in the plume region is approxi mately regarded as uniform rectilinear motion in the Particle model. Therefore, the Particle model shall first determine the number of incident beam ions in the unit time, as well as the velocity reversal distribution an d position distribution at the outlet plane.

The number Δn_i of Xe^+ ion erupted from the outlet within unit time step Δt can be obtained by beam cu rrent I_{ei}:

$$\Delta n_i = I_{ei}\Delta t \quad (7)$$

The beam ions velocity v_{bi} is also calculated by Eq. (2).The initial velocity direction of the beam ion is expressed as $(v_i;\alpha_1;\alpha_2)$ in the spherical coordinates (as shown in Fig. 2), where α_o is the divergence ang le; α_1 is the angle between the component of the initial velocity $\vec{v}_i$ on the XY plane and the X axis, which i s equal to the angle between the position vector $\vec{r}$ on the outlet plane and the X axis; α_2 is the angle betwee n the initial velocity $\vec{v}_i$ and the Z axis, which changes between ($0 \sim \alpha_o$):

$$\alpha_2(r) = \frac{\alpha_o}{r_o} r \quad (8)$$

Where, r_o is the outlet radius of thruster; and r is the distance between ion and outlet axis.

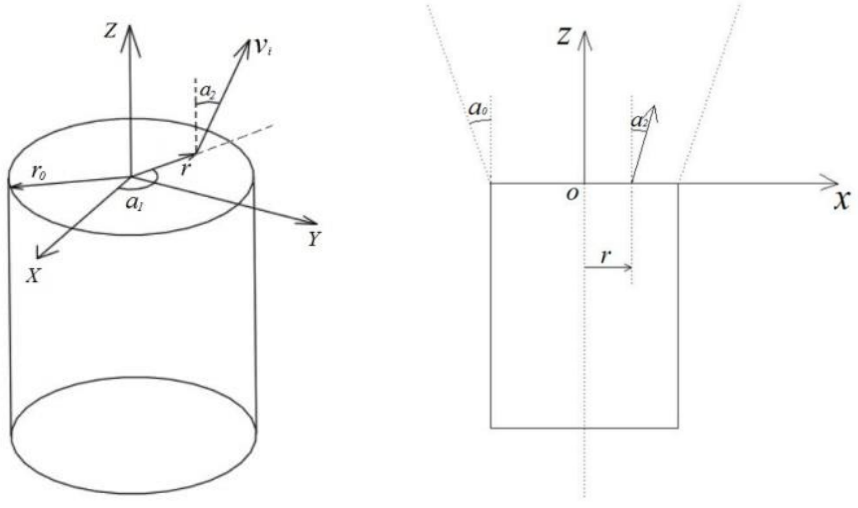

a)XYZ 3D image b)XZ 2D section image

Figure 2. Establishment of spherical coordinates describing the velocity reversal of ion

The beam current density of the traditional ion thruster is high at the outlet center of the thruster and lo w at the edge[16], so the initial position of the Xe^+ ion shall be accordingly distributed based on the Eq. (1). T

herefore, in the Particle model, this paper proposes the central distribution of the initial position of Xe^+ ion according to the analytical Eq. (1).

Since the analytical model of beam current density can ensure that the beam current at the outlet plane o f the thruster is approximately equal to I_{ei}, it can be ensured that the total number Δn_i of Xe^+ ion ejected f rom the outlet within the unit time step Δt is constant.

3) Comparison of simulation results of beam ion

Taking the divergence angle of 7.5 °as an example, we compare the beam ion number density distributi on of analytical model and the Particle model. Fig. 3 shows the number density distribution of the beam io n. It can be seen that the Particle model agrees well with the simulation results of the analytical model. Fig. 4 and 5 show the variation trend comparison of the simulation results of the two models in the axial and rad ial directions. It can be seen that the distribution of the two are basically the same, which indicates that the Particle model can also simulate the distribution of the beam ion well.

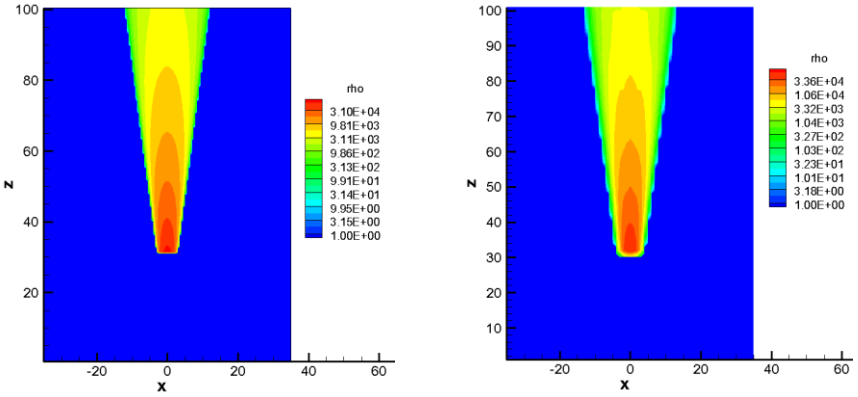

a)Analytical model b)Particle model

Figure 3. Comparison of the number density of beam ion

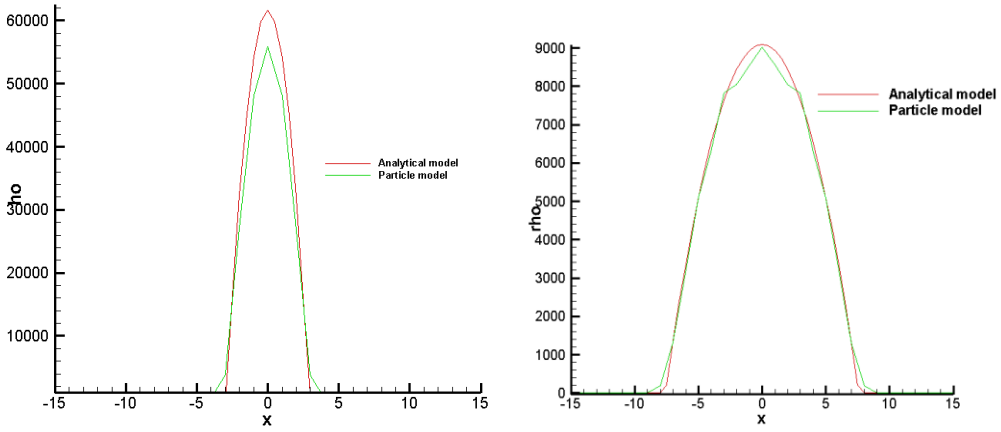

a) Outlet of thruster b) 20cm at the downstream thruster

Figure 4. Radial distribution of the number density of beam ion

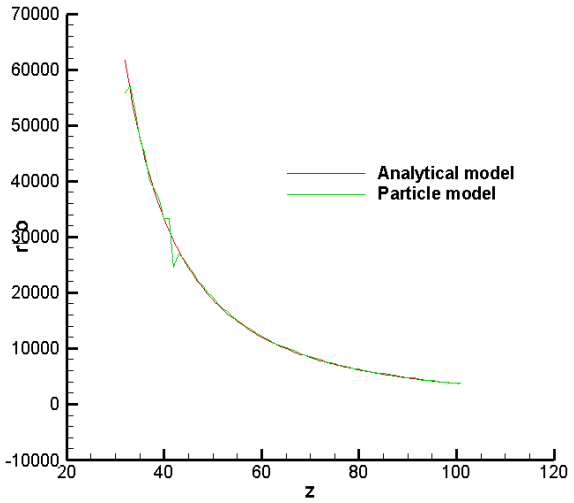

Figure 5. Number density distribution of beam ion of outlet axis

III. CEX Ion Simulation Model

In this section, the simulation method and flow of the generation and the motor process of CEX ion are briefly introduced. Then, the simulations of the analytical model and the 3D full particle model simulation are used respectively to obtain the beam current ion distribution, neutral atom distribution and CEX ion distribution of NSTAR ion thruster. Finally, the simulation results of the two models are compared and the correctness and accuracy of the 3D full particle model are verified.

(1) Introduction of CEX collision model

In addition to the beam ion distribution, the distribution of the neutral atoms of plume should be obtained. In the analytical model, the distribution of neutral atoms still obeys the point-source model[5]. In the 3D full particle model, the neutral atom is obtained by DSMC method simulation, and the detailed description of DSMC algorithm is shown in the Ref. 6. After the distribution of the beam current ion and the neutral atom are obtained, the generation process of CEX ion can be simulated by MCC algorithm. For analytical model, CEX collision can only be simulated by Standard MCC. In the full particle model, two collision algorithms (Standard MCC and P-null MCC) can be used for simulation, but in order to compare with the analytical model, Standard MCC is used to simulate CEX collision in the 3D full particle model in this section. The movement process and position tracking of CEX ion are simulated by IFE-PIC algorithm.

So the CEX ion simulation process is divided into three steps:

1) Simulation of the beam ions with analytical model or Particle model.

2) Simulation of neutral flow exhausted from the ion thruster with analytical model or DSMC model.

3) Simulation of the CEX ions around NSTAR using IFE-PIC-MCC model and beam ions and neutral flow obtained above, respectively. In the Standard MCC method, the volumetric generation of CEX ions is calculated with the following equation:

$$N_{CEX} = n_n n_b v_b \sigma_{CEX}\left(v_b\right) \tag{9}$$

Where n_n and n_b are the neutral and beam ion densities, v_b is the beam ion velocity, and σ is the velocity dependent CEX cross section;

(2) Comparison of CEX ion simulation results

The operational parameters of NSTAR ion thruster and the experimental data of its plume CEX ions used by the simulation in this section are derived from Ref. 7. The simulation conditions are operating conditions ML 83 and the divergence angle is 15 °.

Fig. 6 shows the simulation results of the beam current ion. It can be seen that the simulation results of t he two models still coincide well at the divergence angle of 15 °. Fig. 7 shows the simulation results of the n eutral atom. It can be seen that the simulation results of the two models coincide well in the near-field regio n. In the far-field region, the neutral atom density of the analytical model is larger than that of the DSMC m odel.

Fig. 8 and Fig. 9 are the simulation results of the CEX ion of the analytical model and 3D full particle m odel respectively. It can be seen that the CEX ion number density of the 3D full particle model coincides w ell with the analytical model in the near field region, but it is smaller than the simulation result of the analyt ical model in the far field region. Obviously this is caused by the difference between the neutral atomic sim ulation results of the DSMC model and the analytic model in the far field region.

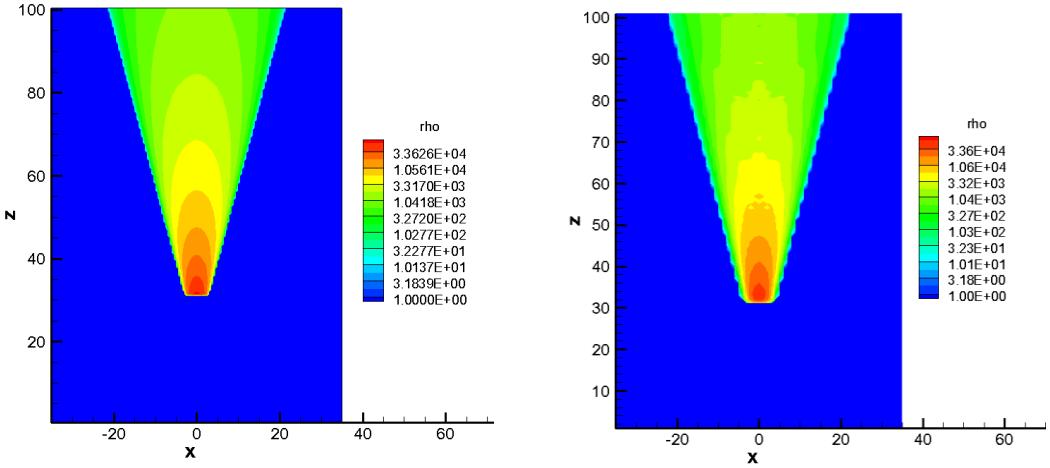

a) Analytical model b) Particle model

Figure 6. Beam current ion simulation results

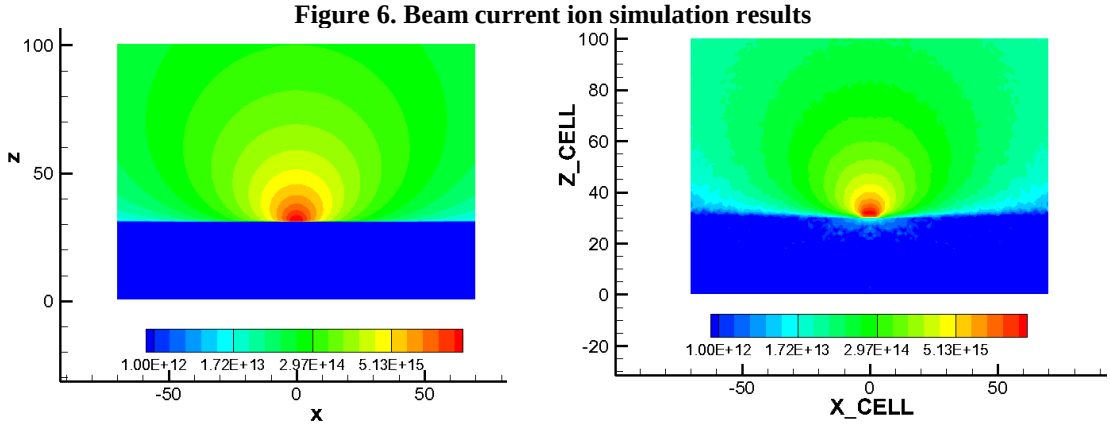

a) Analytical model b) DSMC model

Figure 7. Neutral atom simulation results

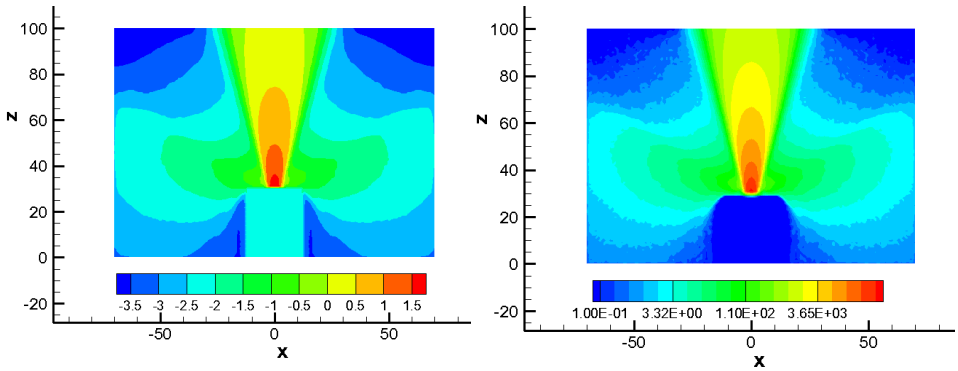

a) CEX ion potential profile b) CEX ion density profile

Figure 8. Simulation results of CEX ion of analytical model

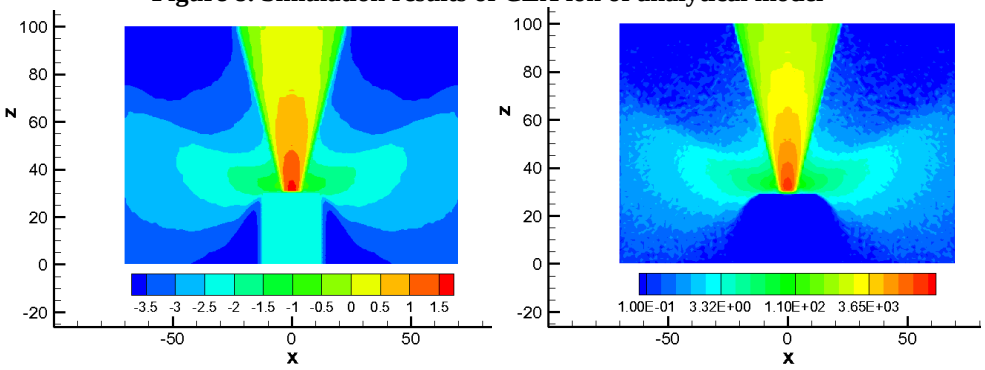

a) CEX ion potential profile b) CEX ion density profile

Figure 9. Simulation results of 3D full particle model

Table 1 lists the simulation results and experimental data of both models. Among them, the measurement position and the collection position of the data point of the simulation results are the radial position with a distance of 75cm from the thruster outlet. It can be seen that the simulation results of 3D full particle model coincides well with the analytical model and experimental data, indicating that the model also has certain accuracy.

Table 1. Measured value of CEX ion of NSTART plume[7]

TypeML83	CEX ion density ($10^{12}m^{-3}$)	Current density ($10^{-3}A/m^2$)
Analytical model	1.4	1.5
3D full particle model	1.2	1.0
Measured value	1.2-4.4	0.9-3.3

IV. Simulation results and analysis of annular ion thruster

The geometric structure of the annular ion thruster is greatly different with that of the traditional ion thruster and is similar to that of the Hall thruster[8], so that the analytical model is no longer applicable. Therefore, 3D full particle model is used to simulate the plume of the annular ion thruster in this section, in order to research the characteristics of the plume distribution of the annular ion thruster and illustrate the universality of 3D full particle model.

(1)3D full particle model of annular ion thruster

In 3D full particle model of the annular ion thruster, CEX collision model is the same as the traditional i on thruster exactly. The DSMC model of the neutral atom is basically the same as that of the traditional ion thruster. The only difference is that the exit plane becomes an annular surface.

However, in addition that the calculation method of Δn_i and v_i is the same as that of the traditional ion t hruster, the beam ion Particle model of the annular ion thruster has two differences from the traditional ion thruster:

1) Because the beam current has two divergence angles (inner divergence angle α_i and outer divergenc e angle α_o),its direction distribution of the initial velocity is different from that of the traditional ion thrust er. As shown in Fig. 10, the initial velocity direction of its beam ion can still be expressed as $(v_i;\alpha_1;\alpha_2)$ un der the spherical coordinates and the meanings of α_1 and α_2 are the same as the descriptions in Section II. T he difference is that the value of α_2 changes between the inner divergence angle and the outer divergence a ngle ($-\alpha_i \sim \alpha_o$):

$$\alpha_2 = \frac{\alpha_o + \alpha_i}{r_o - r_i}(r - r_i) - \alpha_i \tag{10}$$

Where, r_o is the external radius of the outlet of thruster and r_i is the internal radius of the outlet of thruste r.

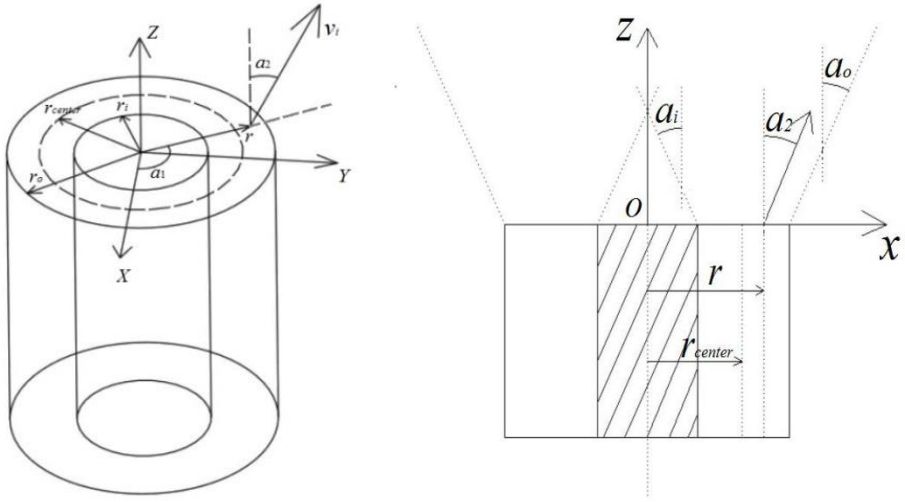

(a)XYZ 3D image (b)XZ 2D section image

Figure 10. Depiction of the spherical coordinates of the beam current ion velocity reversal of the ion thruster

2) There is no corresponding analytical model of the beam distribution for the annular ion thruster. How ever, in the exit plane of the annular ion thruster, the beam current density at $r = r_{center}$ is still higher[17-18]. Th erefore, we assume that the initial position of the beam current ion of the annular ion thruster is also subject to the central distribution, and its beam ion distribution is still subjected to the point-source model, as show n in Fig. 11.

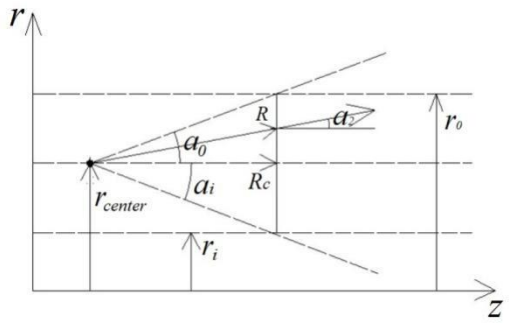

Figure 11. Schematic diagram of point-source model of beam current of annular ion thruster

Therefore, the beam density distribution of the outlet plane of the annular ion thruster can be constructe d according to the analytical Eq. (1),

$$j_{bi}(R,\alpha_2) = Aev_{bi}\bar{n}_{bi0}(\frac{R_c}{R})^2(1-\frac{\alpha_2^{\ 2}}{\alpha_{i,o}^{\ 2}}), -\alpha_i < \alpha_2 < \alpha_o \qquad (11)$$

Where, $\bar{n}_{bi0}$ is average beam current density, $\bar{n}_{bi0} = \frac{I_b}{ev_{bi}\pi\left(r_o^{\ 2} - r_i^{\ 2}\right)}$; $R = R_c/\cos\alpha_2$; $\alpha_{i,o} = \begin{cases} \alpha_i, -\alpha_i < \alpha_2 < 0 \\ \alpha_o, 0 \le \alpha_2 < \alpha_o \end{cases}$.

It is worth noting that in Eq. (11), it is necessary to set the coefficient A to ensure that the beam curren t at the annular ion thruster exit is still equal to I_{ei}.

(2) Simulation results and analysis

The design parameters of the annular ion thruster are shown in Table 2. Among them, the beam current is 1.6A; the inner divergence angle and the outer divergence angle are 15 °, and the coefficient A is 1.5; the ionization rate is 90%.

Table 2. Operational parameters of annular ion thruster

Parameters (units)	Numerical values
Voltage U_{acc} (V)	1800
Beam current I_i(A)	>1.6
Outer divergence angle (α_o)	<15 °
Inner divergence angle (α_i)	<15 °
Mass rate (mg/s)	2.52
Specific impulse (s)	>5000
Ionization rate	>90%
Outer diameter r_o(mm)	225
Inner diameter r_i(mm)	126
Neutral atomc temperature (K)	500
Electron temperature T_e(eV)	2

Fig. 12 shows the simulation result comparison of the beam current ion of the annular ion thruster. It ca n be seen that the distribution of the beam current ions of the annular ion thruster changes greatly compared with that of the traditional ion thruster. The beam currents are overlapped in the axis area, so the beam den sity is higher in axis region than in the wing area. And the layering of the beam current density along the ax is direction is not obvious. Fig. 13 shows the radial distribution of the density of the beam current ion numb er. It can be seen that the radial distribution of the beam ions of the annular ion thruster in the near field reg ion shown M-shape.

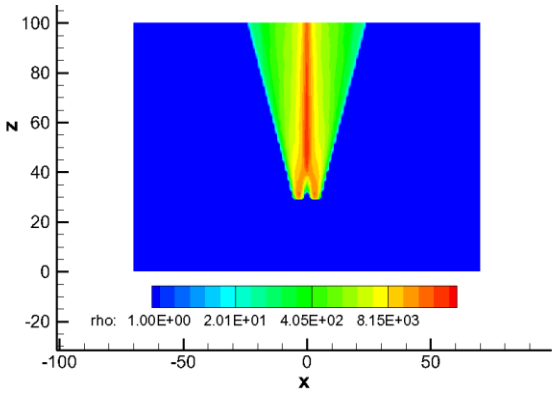

Figure 12. Beam ion number density distribution

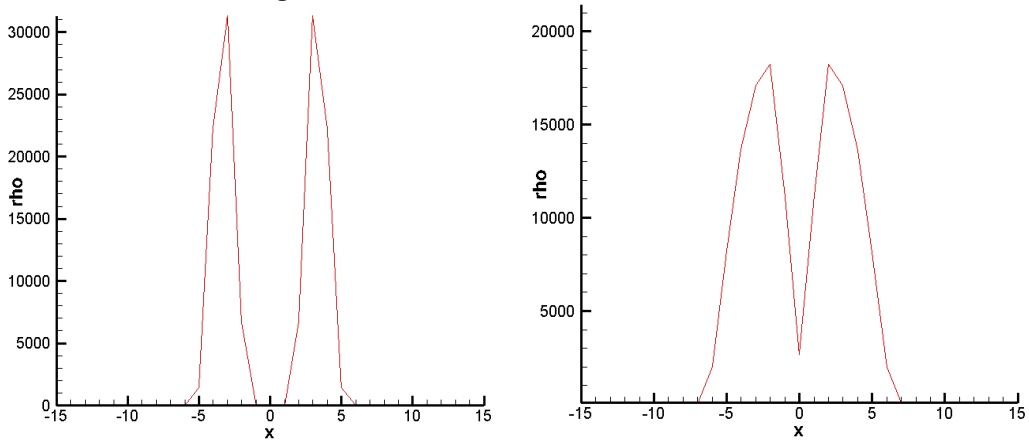

a) Thruster outlet b) 20cm at the downstream thruster

Figure 13. Radial distribution of beam current ion number density

Fig. 14 shows the simulation results of the neutral atom and CEX ions of the annular ion thruster. It can be seen from Fig. 14 a) that the simulation results of the neutral atom distribution of the annular ion thruster is not far from that of the traditional ion thruster. It can be seen from Fig. 14 b) that the distribution of CE X ions has a large gap compared with that of the traditional ion thruster, and the potential and density distri bution of CEX ions in the near field region exhibit a wave-like distribution. It can be seen from Fig. 13 that this is because the beam current distribution in the near field region is in M-shape with high-low conversion in the radial direction, so that the distribution of the CEX ions diffused from the near field region is wave-l ike eventually.

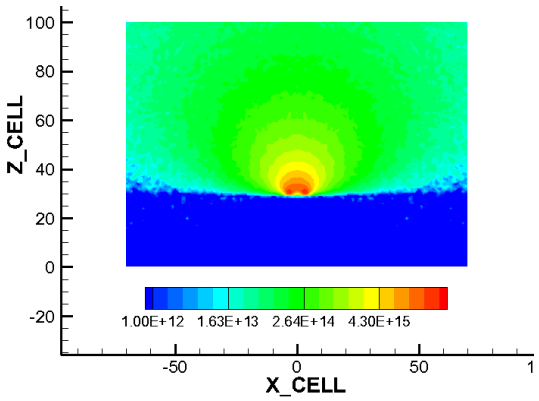

a) Neutral atom density distribution diagram

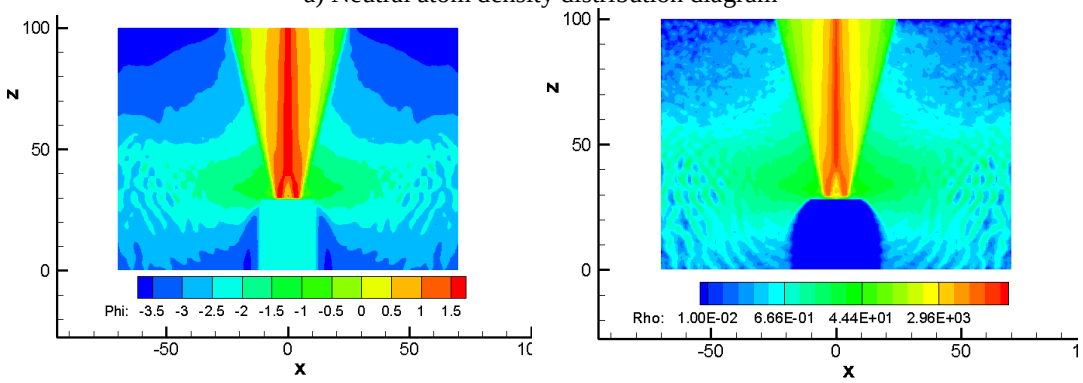

b) CEX ion potential (left) and number density (right) distribution

Figure 14. Simulation results of plume of annular ion thruster

V. Conclusion

The CEX ion simulation results of NSTAR ion thruster show that the simulation results and experimental data of the 3D full particle simulation model and analytical model coincide well, which shows that the 3D full particle simulation model can also simulate the plume distribution of ion thruster well. In the 3D full particle model of the annular ion thruster, the DSMC model and the CEX collision model are basically the same as the corresponding 3D full particle sub-model of the traditional ion thruster. For the Particle model, we propose a corresponding central distribution method based on the analytical model. The results show that the beam current of the annular ion thruster changes greatly compared with that of the traditional ion thruster, and the number density of the beam current ion is high at the axis and low in the two wings, and is in M-shape in the radial direction in the near field region. Although the results of neutral atom simulation of annular ion thruster are not far from that of traditional ion thruster, the simulation results of CEX ion are also different due to the large difference in beam distribution. There is a wave-like distribution in the near field region.

VI. Acknowledgements

This research work is supported by Program of Shenzhen Technology Projects (JCYJ20160226201347750, JCYJ20170413103337899).

References

[1]Samanta Roy R I, Hastings D E. Modelling of Ion Thruster Plume Contamination[C]// Joint Propulsion Conferenc e and Exhibit. Washington, D.C: The Press of Institute of Aeronautics andAstronautics, 1993：12-19.

[2]Stephani K A, Boyd I D, Balthazor R L, et al. Analysis and Observation of Spacecraft Plume/Ionosphere Interactio ns During Maneuvers of the Space Shuttle[J]. Journal of Geophysical Research: Space Physics, 2014, 119（9）: 7636-7648.

[3]King L B, Parker G G, Deshmukh S, et al. Study of Interspacecraft Coulomb Forces and Implications For Formati on Flying[J]. Journal of Propulsion and Power, 2003, 19（3）：497-505.

[4]Shan K, Chu Y, Li Q, et al. Numerical Simulation of Interaction between Hall Thruster CEX Ions and SMART-1 Spacecraft[J]. Mathematical Problems in Engineering, 2015, 2015(3):1-8.

[5]Roy S .Numerical simulation of ion thruster plume backflow for spacecraft contamination assessment[D]. Boston: Massachusetts Institute of Technology, 1995

[6]Bird G A. Molecular gas dynamics and the direct simulation of gas flows /[M]. Clarendon Press ;, 2003.

[7]Wang J, Brinza D, Young M. Three-Dimensional Particle Simulations of Ion Propulsion Plasma Environment for Deep Space 1[J]. Journal of Spacecraft & Rockets, 2001, 38(3):433-440.

[8]Patterson M，Herman D，Shastry R，et al. Annular-Geometry Ion Engine：Concept，Development Status，an d Preliminary Performance[C]//48thAIAA/ASME/SAE/ASEE Joint Propullsion Conference & Exhibit. 2012：3798.

[9]Tajmar M, Gonz-Uuml J, lez, et al. Modeling of Spacecraft-Environment Interactions on SMART-1[J]. Journal of Spacecraft and Rockets, 2001, 38（3）：393-399.

[10]Markelov G, Gengembre E. Modeling of Plasma Flow Around SMART-1 Spacecraft[J]. IEEE Transactions on Pl asma Science, 2006, 34（5）：2166-2175.

[11]Boyd I D. Numerical Simulation of Hall Thruster Plasma Plumes in Space[J]. IEEE Transactions on Plasma Scien ce, 2006, 34（5）：2140-2147.

[12]R.Kafafy and Y.Cao, “Modelling ion propulsion plume interactions with space craft information flight,” Aero nau tical Journal, vol.114,no.1157,pp.417–426,2010.

[13]R. Kafafy, T. Lin, Y. Lin, and J. Wang, “Three-dimensional immersed finite element methods for electric field si mulation in composite materials,” International Journal for Numerical MethodsinEngineering,vol.64,no.7,pp.940–972,2 005.

[14]J.Wang, Y.Cao, R.Kafafy, J.Pierru, and V.K.Decyk, “Simulations of ion thruster plume-spacecraft interactions on parallel supercomputer,” IEEE Transactions on Plasma Science, vol. 34, no.5,pp.2148–2158,2006.

[15]Wang J, Cao Y, Kafafy R, et al. Electric propulsion plume simulations using parallel computer[J]. Scientific Prog ramming, 2007, 15(2):83-94.

[16]David O，Scott B， Kevin W， et al． Deep Space Mission Applications for NEXT: NASA`s Evolutionary Xe non Thruster［R］． AIAA－2004－3806．

[17]Shastry R，Patterson M J，Herman D A，etal. Current Density Measurements of an Annular-Geometry Ion Eng ine[C]//Proc 48thAIAAJointPropulsionConf.（Atlanta，GA，2012.

[18]Patterson M J, Foster J E, Young J, et al. Annular Engine Development Status[C]// Aiaa/asme/sae/asee Joint Prop ulsion Conference. 2013.